

13. LATE PLEISTOCENE DISSOLUTION CYCLES IN THE VANUATU REGION, WESTERN PACIFIC OCEAN¹

J. Ignacio Martínez R.²

ABSTRACT

A high-resolution record of foraminiferal fragmentation (a dissolution indicator) for the last 250 k.y. (isotopic Stages 1 to 7) is identified in the upper 61.9 m of Ocean Drilling Program (ODP) Hole 828A, west Vanuatu. This record is comparable in detail to the atmospheric CO₂ record and the δ¹⁸O stack. Phase shifts between preservation spikes and maximum ice volumes (δ¹⁸O of *Globigerinoides sacculifer*) are analogous to those on Ontong Java Plateau. Mass spectrometer (AMS¹⁴C) dating of a sample taken at the base of dissolution cycle B1 and the position of the last glacial maximum indicates a lag in time of ~8 k.y. in the Vanuatu region for the last glacial termination. When dissolution spikes are compared with minimum ice volumes there is no phase shift for the last two glacial terminations. The difference between Vanuatu and Ontong Java Plateau may be explained by local CO₂ sinks and the interplay between intermediate and deep water masses. Terrigenous input increasingly affected sediment of Hole 828A on the North d'Entrecasteaux Ridge (NDR) as it approached Espiritu Santo Island. Mud and silt suspended in mid-water flows become important after 125 ka, while turbidites bypass the New Hebrides Trench only towards the last glacial maximum (LGM). Terrigenous supply seems to affect the lysocline profile that changed from an "open ocean" to a "near continent" type, thus favoring dissolution. Fragmentation of planktonic foraminifers is a more sensitive indicator of lysocline variations than is foraminiferal susceptibility to dissolution, the foraminiferal dissolution index, the abundance of benthic foraminifers, or CaCO₃ content. A modern foraminiferal lysocline for the neighboring area (between 10°S and 30°S, and 160°E and 180°E) is found at 3.1 km below sea level, compared to west Vanuatu where it is shallower. The past lysocline level was deeper than 3086 m during intervals of dissolution minima, and ranged from ~2550 to 3000 m during intervals of dissolution maxima. The high sedimentation rates (in the order of 10 to 50 cm/k.y.) found in Hole 828A offer a great potential for future high-resolution studies either in this hole or other western localities along the NDR. Areas of high sedimentation near continental regions have been discarded for paleoceanographic and/or paleoclimatic studies. Nonetheless, conditions analogous to those found in Hole 828A are expected to occur in many trench areas around the world where mid-water flows have preserved as yet undiscovered fine high-resolution sedimentary records.

INTRODUCTION

Late Pleistocene paleoceanographic studies of the western equatorial Pacific are widely available (Berger and Killingley, 1977; Berger, 1977; Wu et al., 1991). A well-established isotopic record (Shackleton and Opdyke, 1973, 1976) and the pattern of CaCO₃ dissolution cycles (Thompson and Saito, 1974; Thompson, 1976) are of particular interest: they are not only of stratigraphic value, but also form the basis of intensive discussion concerning the oceanic geochemical response to CO₂ change during glacial-interglacial cycles (e.g., Broecker, 1971). A time lag between the isotopic and dissolution records was observed in several equatorial Pacific cores whose water depth is near, or deeper than the lysocline (Luz, 1973; Luz and Shackleton, 1975; Shackleton and Opdyke, 1976). Maximum preservation tends to occur during deglaciations and minimum preservation tends to occur during ice build-up (for a review see Farrell and Prell, 1989). The time lag between preservation maxima and glacial terminations has been estimated to vary between 3 and 20 k.y. (Luz and Shackleton, 1975; Shackleton and Opdyke, 1976; Moore et al., 1977; Berger, 1977; Farrell and Prell, 1989; Le and Shackleton, 1992).

Most western equatorial Pacific studies concentrate on the Ontong Java Plateau north of the Solomon Islands and more recently in the Sulu Sea, where high sedimentation rates offer the opportunity to examine higher-frequency oceanographic and climatic changes (Linsley and Thunell, 1990; Kudrass et al., 1991; see Fig. 1 for the location of Ontong Java Plateau). South of these regions a few paleoceanographic studies have been undertaken (e.g., Moore et al., 1980;

Anderson et al., 1989) but these do not deal with dissolution. Paleotemperature estimates by Anderson et al. (1989), using the modern analog technique (MAT), are similar to CLIMAP (1981) results for the equatorial west Pacific, north of 25°S, but are significantly different further south. Temperatures for the southern Coral Sea during the last glacial maximum (LGM) are reported by Anderson et al. (1989) to be 3° to 4°C colder than present day, and the East Australian current may not have existed or was weaker than today.

The present study analyzes cores from Holes 828A and 832A drilled west of Vanuatu. In this region dissolution effects interfere with paleoclimatic estimates based on faunal analysis at least for interglacial periods (findings consistent with Thompson, 1976), but the high sedimentation rate in Hole 828A offers great potential for studying the effects of dissolution and dissolution time lags. These cores display great differences in lithology, sedimentation rates, terrigenous content, and foraminiferal preservation. Consequently, the aim of this paper is to show these differences, to compare this information with previous results from the Ontong Java Plateau, and to discuss a possible mechanism for the dissolution cycles in the western equatorial Pacific.

Dissolution Cycles

Dissolution of planktonic foraminifers in the deep sea has been studied extensively (Berger, 1968, 1970; Thompson and Saito, 1974; Shackleton and Opdyke, 1976; Thunell, 1976; Thunell et al., 1992), and the dissolution pattern through the Pleistocene is well established for the equatorial Pacific. Dissolution fluctuates with glacial and interglacial periods (Arrhenius, 1952; Hays et al., 1969), and generally is greatest during interglacials (odd-numbered isotopic stages). This may provide a basis for regional correlation (Thompson and Saito, 1974). As mentioned above, comparison of carbonate records with δ¹⁸O isotopic records show regional variations of their phase

¹ Greene, H.G., Collot, J.-Y., Stokking, L.B., et al., 1994. *Proc. ODP, Sci. Results*, 134; College Station, TX (Ocean Drilling Program).

² Australian National University, Department of Geology, Australian Marine Quaternary Program, GPO Box 4, Canberra ACT 2601, Australia.

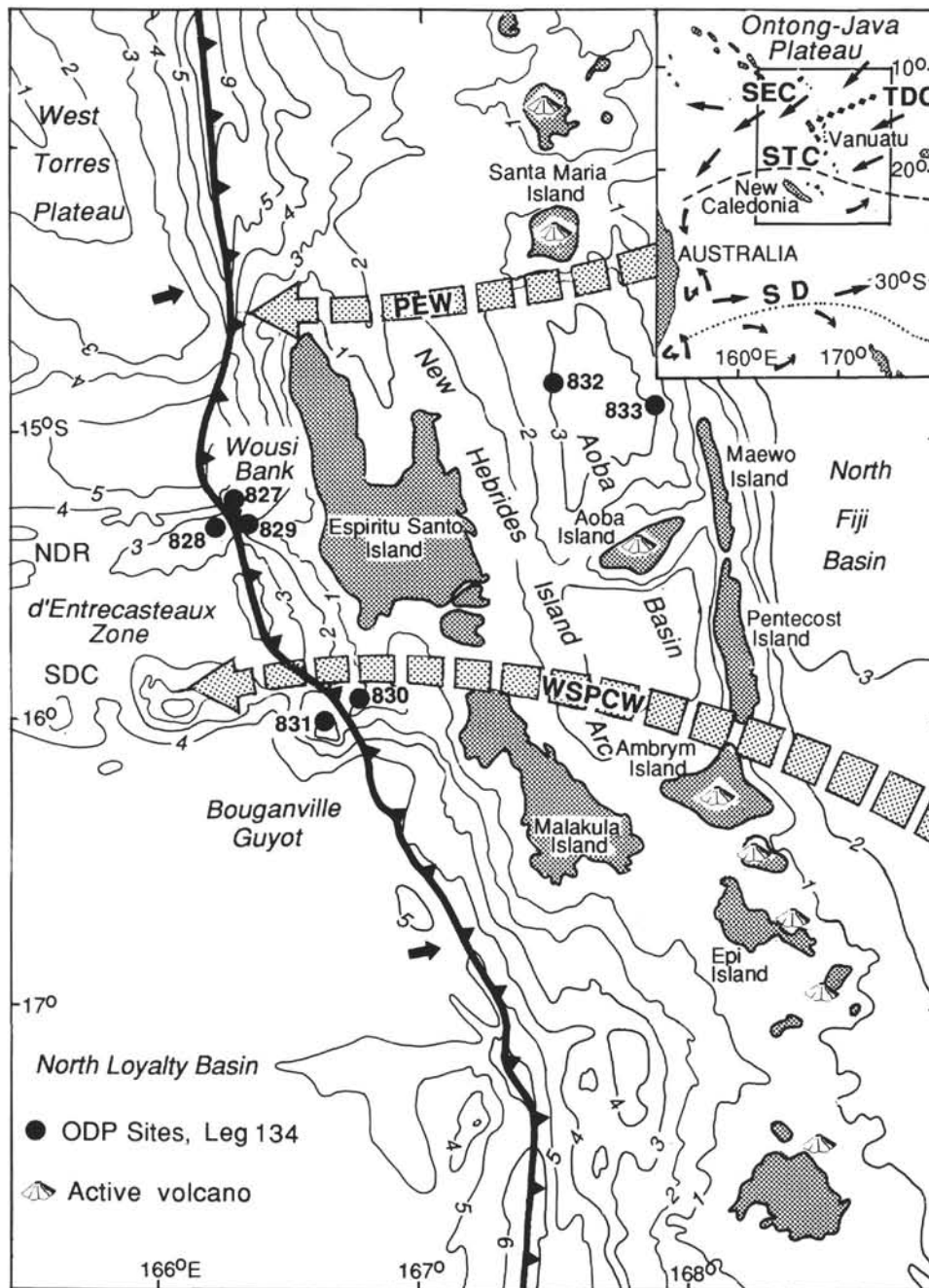


Figure 1. Location map and selected oceanographic features. Note the location of Site 828 west of the North New Hebrides Trench. Surface currents (insert, based on Rotschi and Lemasson, 1967): SEC = South Equatorial Current, TDC = Trade Drift Convergence, STC = Southern Tropical Convergence, SD = Subtropical Divergence. Water masses pathway (after Tomczak and Hao, 1989): PEW = Pacific Equatorial Water, WSPCW = West South Pacific Central Water. Bold line with teeth = New Hebrides Trench, NDR = North d'Entrecasteaux Ridge, SDC = South d'Entrecasteaux Chain. Bathymetry in kilometers.

relationships; however, carbonate maxima and minima often correspond to transitional stages in the climatic cycles rather than to glacial maxima or minima (for a review see Moore et al., 1977; Farrell and Prell, 1989). Lags between the isotopic and the dissolution curves show geographical variations that prevent correlation beyond a local region (i.e., the equatorial Pacific).

Three different criteria are used to define the lag time: (1) the difference in age between glacial terminations (the mid-point between the maximum and minimum ice volumes from the $\delta^{18}\text{O}$ record) and

the mid-point between dissolution minima and maxima (e.g., Luz and Shackleton, 1975); (2) the difference between ice volume minima and dissolution maxima (Le and Shackleton, 1992); and (3) the difference between ice volume maxima and dissolution minima (e.g., Moore et al., 1977). Furthermore, differences in sedimentation rates, stratigraphic resolution, and techniques applied to the study of different cores may influence the accuracy of the recorded time lag between these geochemical events. Even the $\delta^{18}\text{O}$ record is modified by dissolution in such a way that "climate optima" (as defined by the

lightest $\delta^{18}\text{O}$ values) tend to shift toward preservation spikes, while apparent "glacial maxima" (characterized by the heaviest $\delta^{18}\text{O}$ values) shift toward dissolution spikes (Wu and Berger, 1989; Wu et al., 1990, 1991).

METHODS

Hemipelagic sediments recovered from Holes 828A and 832A were sampled because they appeared to be less affected by turbidites and volcanic ash than other ODP cores from Leg 134 (Fig. 1 and Table 1). Hole 831A from the Bouganville Guyot, in spite of being dominated by pelagic material, was found to be "soupy" in character (Collot, Greene, Stokking, et al., 1992), and therefore was not studied. High terrigenous and volcanic content, as in sediments of Hole 828A, are generally unsuitable for paleoceanographic studies (Ruddiman, 1977). However, good information was obtained by careful sampling above turbidite sequences, where pelagic sediments dominate. Kudrass et al. (1991) took a similar approach for the Sulu Sea, where hemipelagic layers are interbedded between turbidites protecting them from bioturbation. As shown below, sedimentation rates at Hole 828A vary from 10 cm/k.y. to more than 50 cm/k.y., which means that a sample 2 cm thick represents 40 to 200 yr. These figures may be lower (excluding any unrecognized hiatus or reworking) if we consider the episodic character of sedimentation (Dott, 1983). Because of the high sedimentation rate, a high-resolution record is obtained with a 50-cm sample interval. Two hundred seventeen samples were studied for fragmentation of planktonic foraminifers, 110 for foraminiferal faunal analysis, and 31 for stable isotopes ($\delta^{18}\text{O}$ and $\delta^{13}\text{C}$). In Hole 832A, samples beneath 30 meters below seafloor (mbsf) commonly were found barren of fossils or highly lithified. Eighty-six samples were processed from Section 134-832A-6H-1 to Section 134-832B-40R-1, and of these 66 were either barren or contained poorly preserved specimens.

Approximately 5 to 7 cm³ of each sample were treated with 3% hydrogen peroxide processed in 50-mL jars, sieved through a 63- μm mesh, then dried in an oven at 40°C, and subsequently dry-sieved through a 149- μm mesh. Approximately 300 planktonic foraminifers were obtained with a microsplitter. Accelerator mass spectrometer analyses (AMS¹⁴C) were obtained for two samples from Hole 828A. Specimens were hand-picked, washed in alcohol, and placed in the ultrasonic cleaner for less than 10 s. Alcohol was then washed away with distilled water. Carbon dioxide was produced by reaction with concentrated phosphoric acid, and stored in glass breakseals for AMS measurement. Sample 134-828A-2H-1, 29–31 cm, provided few specimens in the fraction >150 μm ; therefore, additional specimens were picked from the 63- to 150- μm fraction. *Globigerinoides ruber* and *Globigerinoides sacculifer* (shallow planktonic species) were combined in Sample 134-828A-2H-1, 29–31 cm, because they give similar AMS¹⁴C results (Broecker et al., 1989).

The $\delta^{18}\text{O}$ record was obtained from *G. sacculifer*. Each sample comprises approximately 7 specimens, selected and cleaned using the same technique as AMS¹⁴C described above. When necessary, a needle was applied to break specimens in which the last chamber was infilled with clay lumps impossible to remove by ultrasonic cleaning. The 150- to 250- μm fraction was selected to obtain young individuals (as they live in the upper photic zone for 7–8 days before sinking to reproduce; Erez et al., 1991), which should give sea surface $\delta^{18}\text{O}$ values. Analyses were carried out using a Finnigan-MAT 251 mass spectrometer at the Research School of Earth Sciences (The Australian National University) with sample dissolution effected with an on-line "acid on individual carbonate" preparation device. Oxygen and carbon isotopic data are reported in " δ " notation relative to the Pee Dee belemnite (PDB) standard.

Dissolution Indicators

Dissolution intensity was assessed from fragmentation of planktonic foraminifers (Berger, 1970), the relative frequencies of solution-

Table 1. Hole locations, water depths, and last occurrence (LO) of *G. ruber* (pink variety).

Sample (cm)	Position		Water depth (m)	Depth of <i>G. ruber</i> LO (pink) (mbsf)
	Latitude	Longitude		
134-828A-5H-5, 59–60	15°17.34'S	166°017.04'E	3086.7	40.99
134-832A-4H-1, 79–81	14°47.78'S	167°034.35'E	3089.3	19.30

susceptible vs. solution-resistant planktonic foraminifers (Berger, 1968), the foraminiferal dissolution index (Berger, 1968), and the abundance of benthic foraminifers (Parker and Berger, 1971). These have been suggested to be reliable indicators of dissolution compared to calcium carbonate concentrations, which can be greatly affected by terrigenous dilution (Thunell, 1976). Recently, to emphasize that normally no distinction is made between rates of dissolution and state of preservation, Arrhenius (1988) showed how these indicators provide only a rough estimation of dissolution. He argued that the state of preservation may differ between two samples due to sediment-accumulation rate differences, even if the rate of dissolution is the same. Later, I shall discuss advantages and disadvantages of the different dissolution indicators in a sequence where sedimentation rates vary from low to high.

The nomenclature of Hays et al. (1969) is used here to designate dissolution (odd numbers) and preservation intervals (even numbers). It has been modified to include dissolution cycles within major intervals, as in B3 (here subdivided into A, B, and C) and B5 (subdivided into A, B, and C).

Fragmentation percentage was determined by counting the number of fragments in a split sample that contained 300 or more whole planktonic foraminifers, and then dividing the number of fragments by the sum of whole planktonic foraminifers together with the number of fragments. An analogous method was used to determine the abundance of benthic foraminifers. The foraminiferal dissolution index (FDX) (Berger, 1968) provides a weighted average of the dissolution rank, as follows:

$$\text{FDX} = \sum (P_i R_i) / r_i$$

where P_i is the percentage of species i , R_i is the rank of species i , and r_i is the mean rank. The solution ranking list given by Bé (1977) is used here.

REGIONAL SETTING

In contrast to the Ontong Java Plateau, the Vanuatu region is affected by higher terrigenous sedimentation (turbidites) and volcanic ashes that easily reach the backarc, the intra-arc, and the forearc areas. In the absence of any major physiographic barrier, clastic sediments from Espiritu Santo Island are spread extensively on the neighboring seafloor. This has a major influence in the central New Hebrides forearc region where the equatorial current flows towards the southwest (Rotschi and Lemasson, 1967). The high number of cyclones in the area (Gray, 1968; Howorth and Greene, 1991) tend to sweep sediments out of the narrow continental shelf of western Vanuatu. The North d'Entrecasteaux Ridge (NDR) on the subducting plate approaches Espiritu Santo Island at a rate of ~13 cm/yr and has done so since about 0.4 Ma (Taylor et al., this volume). Hence sedimentation at Site 828 records the transit from low to high terrigenous input during the latest Pleistocene. The Trade Drift Convergence (TDC) extends southwest-northeast (Fig. 1). This feature apparently coincides with the boundary of two important shallow to intermediate water masses: the Pacific Equatorial Water (PEW) that originates in the central Pacific, and the Western South Pacific Central Water (WSPCW), that is formed at the Subtropical Convergence in the

southern Tasman Sea (Tomczak and Hao, 1989). These water masses have similar salinities with a maximum of 35.9‰ at ~150 m to about 34.5‰ at ~400 m. The Antarctic Intermediate Water (AAIW) occurs at intermediate depths (500 to 1500 m), whereas further below (1500 m to bottom) the Circumpolar Deep Water (CDW) crosses the area (Pacific Deep Water or PDW of Thunell et al., 1992). The CDW derives from the North Atlantic Deep Water (NADW) that mixes with Antarctic waters and is transported around the Antarctic to spread over the deep Pacific and Indian oceans (Broecker and Peng, 1982; Emery and Meincke, 1986).

Hole 828A

Hole 828A was drilled on the North d'Entrecasteaux Ridge (NDR) on a flat, terrace-like feature that projects out from a bathymetric slope, at a water depth of 3086 m (Table 1). Cores 139-828A-1H to -7H cover the upper 62 m of this hole. Samples were taken at intervals varying from 20 to 80 cm from the core top down to 62 mbsf (Fig. 2). The interval sampled comprises lithostratigraphic Unit I which consists of a greenish gray (10Y 4/1) volcanic silt with foraminiferal sand interbeds (see Collot, Greene, Stokking, et al., 1992). Scoured bases are common within the unit while bioturbation is mainly restricted to Cores 4H to 7H. Equally conspicuous is the progressive increase of CaCO₃ from Core 5H to 7H (see Collot, Greene, Stokking, et al., 1992) and the common occurrence throughout the unit of deep benthic and planktonic foraminifers, woody material, few radiolarians, and sponge spicules. These features resemble Facies D1.2 "muddy silts" and Facies C1.1 "poorly sorted muddy sands" of Pickering et al. (1989), even though the presence of contourites is not discarded. The magnetic profile shows a normal polarity for Cores 1H to 7H suggesting that these sediments were deposited during the Brunhes Chron (Collot, Greene, Stokking, et al., 1992). At 61.9 mbsf an unconformity separates the upper Pleistocene from the lower Pliocene (Collot, Greene, Stokking, et al., 1992).

Hole 832A

Hole 832A was drilled in the North Aoba Basin at a water depth of 3089.3 m (Fig. 1). Sampling was restricted to lithostratigraphic Unit I. Sample spacing was 40 cm but sometimes increased up to 150 cm due to the high content of volcanic ash, soupy intervals, and turbidites. Samples below 30 mbsf commonly were barren of fossils or highly lithified. Above this depth 66 of the 86 processed samples were either barren or contained poorly preserved specimens. Lithostratigraphic Unit I (385.6 m thick) is mainly sandy to clayey volcanic silts interbedded with volcanic ash layers, and is restricted to the Brunhes Chron (see Collot, Greene, Stokking, et al., 1992). This array of facies resembles volcanic sedimentation model Type III of Huang (1980), which implies closely spaced volcanic eruptions and a high sedimentation rate.

RESULTS

Chronology of Hole 828A

Based on a preliminary assessment of paleomagnetic data, and the occurrence of *Globorotalia tosaensis* at 61.4 mbsf, Collot, Greene, Stokking, et al. (1992) suggested that most, if not all, of the Brunhes Chron was represented in Hole 828A. Oxygen isotope data reported herein show that the upper 61.9 mbsf includes Stages 1 to 7. *G. tosaensis* and other Pliocene species (e.g., *Dentoglobigerina altispira altispira*, *Globorotalia limbata*, *Sphaeroidinella paenedehiscens*) are iron-stained, and are believed to be reworked. Consequently, at an unconformity at 61.9 mbsf, the upper Pliocene to upper Pleistocene (up to isotopic Stages 8, and possibly part of 7) are missing.

The Pleistocene chronology of Hole 828A is given by the last occurrence of *G. ruber* (pink variety) (Fig. 2B), two AMS¹⁴C dates (Fig. 2B, Table 2), and the δ¹⁸O record of *G. sacculifer* (Fig. 2J,

Table 3). *G. ruber* (pink variety) is a reliable biostratigraphic marker that became extinct at about 120 ka in the Indian-Pacific region (Thompson et al., 1979). In Hole 828A this event corresponds to a δ¹⁸O minimum of -2.36‰ at approximately 40 mbsf. This minimum is assigned to isotopic Stage 5e, and the δ¹⁸O data from 0 to 40 mbsf closely follows the standard δ¹⁸O curve of Martinson et al. (1987). The δ¹⁸O record shows values that vary between -0.61‰ and -2.41‰ (the analysis of the whole set of samples is in progress). Interglacial Stages 1, 5, 7, and glacial Stage 6 can be seen clearly (Fig. 2J), whereas sharp divisions among Stages 2 to 4 are not possible to recognize with the present density of sampling. The δ¹⁸O data indicate that the LGM is at 9.49 mbsf, 1.5 m above AMS¹⁴C (Sample 134-828A-2H-5, 59–61 cm), which gave an age of 16,420 ± 210 ka. The isotopic maximum corresponding to the LGM is 17.6 ka according to the prevailing astronomically tuned chronology (Martinson et al., 1987). The younger age of the δ¹⁸O maximum in Hole 828A may reflect the difference between radiocarbon and astronomical years (about 2 k.y. duration 9 to 20 ka; Bard et al., 1990), or may be due to relatively wide spacing of δ¹⁸O measurements reported here. At this preliminary stage in the analysis, the position of the LGM at 9.49 mbsf appears acceptable; greater precision is expected with a higher sample density in the δ¹⁸O record (work in progress). The positions of glacial Terminations I and II are drawn at the mid-point between δ¹⁸O maxima and minima.

Hole 832A in the North Aoba Basin shows similar results to those obtained from Hole 828A for the upper part of the sequence and, in spite of reworking of foraminifers and the presence of volcanic ash, it is possible to recognize Termination II (suggested by the last occurrence of the pink variety of *G. ruber*; Fig. 3). The last occurrence of *G. ruber* (pink variety), however, is not an abrupt event at ~28 mbsf, but it occurs sporadically above in very low numbers up to 19.3 mbsf. The same pattern was observed by Thompson et al. (1979) in Indian and Pacific ocean cores, where the species has been reported to range most frequently up to isotopic Stage 5e, but in one example from the Indian Ocean ranges up to Stage 4.

Dissolution

The foraminiferal content of most samples was greatly diluted by terrigenous material, particularly in the interval between 0 and 40 mbsf in Hole 828A. Sometimes no more than 400 specimens (>150 μm) could be recovered from 5-cm³ samples.

Figure 2 shows the faunal content of Hole 828A. Plots of the most common species are arranged from left to right according to increasing dissolution resistance and are compared against the percentage of fragmentation and the stable isotope record. Fragmentation as well as the percentages of benthic foraminifers show high values during interglacial Stages 1 and 5. Fragmentation also shows two peaks in the 50- to 60-m interval, which is assigned to interglacial Stage 7. There is some correspondence between high percentages of benthic foraminifers and high fragmentation values (Fig. 2I). Boundaries of carbonate dissolution Intervals B1 to B5 (nomenclature from Hays et al., 1969) are identified where fragmentation values change abruptly or exceed the 20% level (Fig. 2E, Table 4). This value corresponds to

Table 2. Accelerator mass spectrometer (AMS¹⁴C) datings on samples from Hole 828A.

Core, section, interval (cm)	Specimens (N)	Size fraction (μm)	Age (yr)	Lab no.
134-828A-2H-1, 29–31	~200 (<i>G. ruber</i>)	>63		
	~100 (<i>G. sacculifer</i>)	>150	9,790 ± 150	NZA 1931
2H-5, 59–61	~240 (<i>G. sacculifer</i>)	>150	16,420 ± 210	NZA 2037

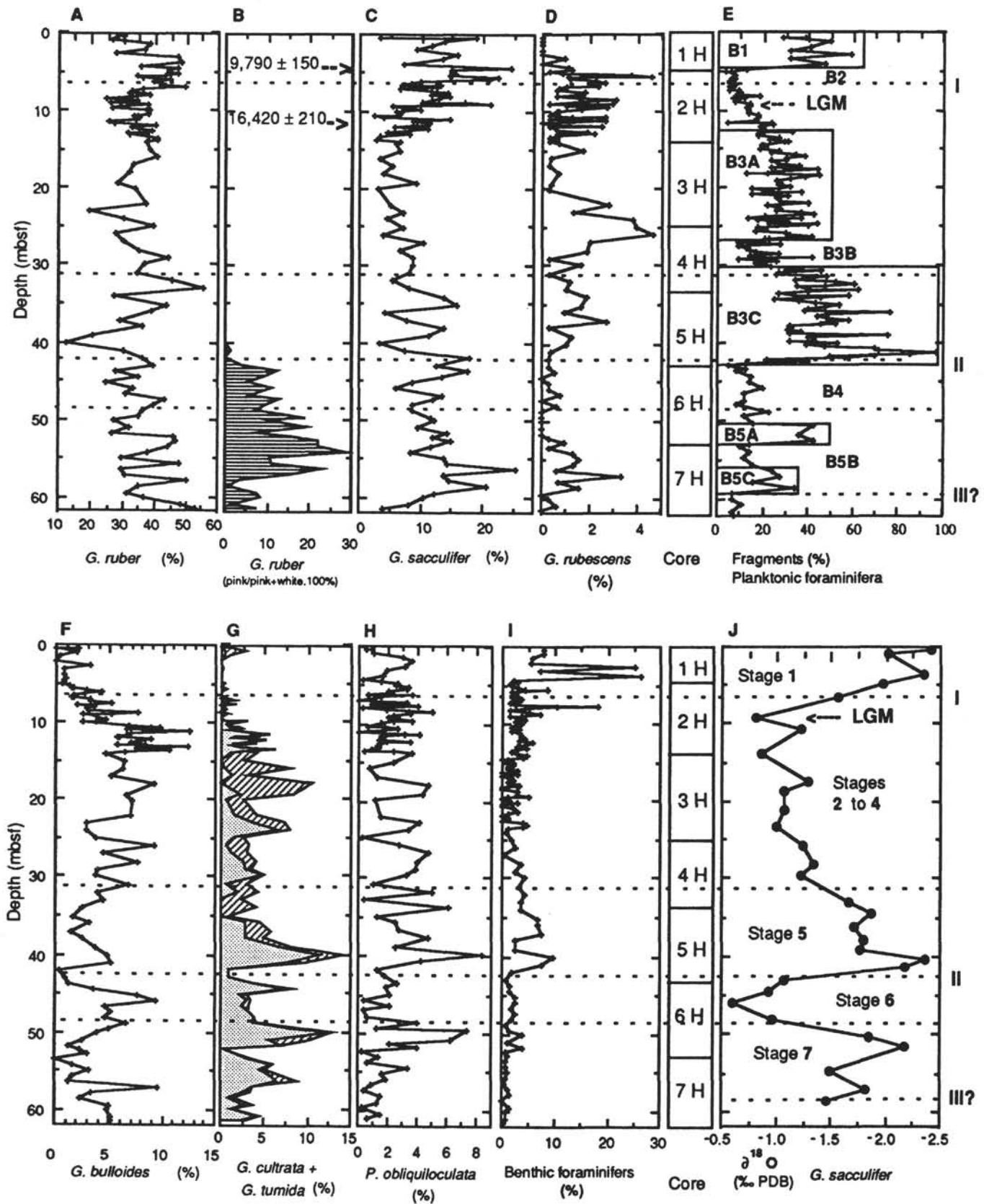


Figure 2. Hole 828A. Percentage variation of selected species of planktonic foraminifera (arranged according to their solution susceptibility) vs. the percentage of planktonic fragmentation (E), benthic foraminifera (I), and the $\delta^{18}\text{O}$ record on *G. sacculifer* (J). B1 to B5 refer to dissolution cycles (nomenclature from Hays et al., 1969), and I to III? refer to glacial terminations. LGM = last glacial maximum. Note the last occurrence of *G. ruber* (pink variety) at 40 mbsf and the two AMS¹⁴C datings (panel B).

the approximate position of the lysocline level in the region as will be shown below.

The dissolution interval boundaries in Hole 828A have a similar relationship to oxygen isotope stages as identified by Shackleton and Opdyke (1976); for example, the B1/B2 boundary is close to the Stage 1–2 boundary, and B3C/B4 is close to the Stage 5e–6 boundary. Dissolution Intervals B3 and B5 are subdivided, in this chapter, on the same basis as major stage boundaries.

Different dissolution indicators (fragmentation, foraminiferal susceptibility, foraminiferal dissolution index, and abundance of benthic foraminifers) are compared in turn as follows:

1. Fragmentation shows a pattern that closely resembles the $\delta^{18}\text{O}$ stack record (Martinson et al., 1987). Greater ranges of fragmentation values (20% to 30%) occur during periods of maximum dissolution and can be attributed to noise and/or normal variations below the lysocline level. During intervals of dissolution minima values range <10%.

2. Variations in foraminiferal species susceptibility show some correspondence with fragmentation percentage: sharp troughs in the solution-susceptible species abundance (e.g., *G. ruber* and *G. sacculifer*; Figs. 2A and 2C, respectively) and sharp peaks in solution-resistant species (e.g., *Globorotalia cultrata*–*Globorotalia tumida* and *Pulleniatina obliquiloculata*; Figs. 2G and 2H, respectively) generally match peaks in fragmentation percentage (Fig. 2E, Table 4). This pattern, however, does not apply to the entire record as peaks in solution-susceptible species sometimes correspond to high fragmentation values. Relative abundances of planktonic foraminifers are not only the product of dissolution, but of paleoclimate and paleoecological conditions in the upper water column.

3. The FDX curve is shown in Figure 4C. We would expect the FDX to follow a similar pattern to that depicted by fragmentation: higher values during dissolution intervals and lower values during preservation intervals. This pattern seems to apply below Termination II only; above it, values fluctuate between 0.65 and 0.86, except for a high peak (1.0) at the base of dissolution Interval B3 (Fig. 4). Similarly to the foraminiferal susceptibility, the foraminiferal dissolution index reflects not only dissolution but is also influenced by paleoclimate and foraminiferal paleoecology.

4. The abundance of benthic foraminifers shows some correspondence with dissolution intervals (values higher than 1%), but occasional anomalously high values are present during intervals of dissolution minima (e.g., during dissolution Interval B2). The abundance of benthic foraminifers reflects, therefore, not only dissolution but other factors such as paleoecological conditions of the seafloor.

From the above discussion it follows that planktonic foraminiferal fragmentation is the most sensitive dissolution indicator and will be further discussed below.

For Hole 832A, dissolution intervals are determined in the same fashion as for Hole 828A, using solution-susceptible vs. solution-resistant species, and where fragmentation percentage exceeds 15%. This stratigraphy should be considered preliminary in the absence of the stable isotope record. The climatic/paleoecologic signal in this hole is highly distorted by sedimentological processes because anomalous percentages (e.g., high percentages of *G. sacculifer* coinciding with high percentage fragmentation, Fig. 3) were present. This also applies to the percentage of benthic foraminifers since they also do not coincide with test fragmentation. Test fragmentation in Hole 832A does not exceed 25% and hence is significantly lower than in Hole 828A.

Relationship of Dissolution and Isotope Stages

Dissolution Interval B1 as well as Interval B3C begin abruptly after preservation Intervals B2 and B4, respectively (Fig. 2E). Dissolution Interval B1 is Holocene in age (~10 ka to present) and is preceded by dissolution minimum B2 that corresponds to the isotope Stage 2–1 transition. The same pattern applies to the Stage 6–5

Table 3. Oxygen and carbon isotope data (per mil deviations from the PDB standard) for *Globigerinoides sacculifer*.

Core, section, interval (cm)	Depth (mbsf)	Specimens (N)	Planktonic foraminifers	
			$\delta^{18}\text{O}(\text{‰})$	$\delta^{13}\text{C}(\text{‰})$
134-828A-				
1H-1, 44–46	0.45	3	-2.41	1.82
1H-1, 106–108	1.06	7	-2.02	0.14
1H-3, 82–83	3.82	7	-2.35	0.73
2H-1, 47–49	4.87	7	-1.97	0.02
2H-2, 79–81	6.69	8	-1.56	0.19
2H-4, 59–61	9.49	8	-0.81	0.09
2H-5, 59–61	10.99	8	-1.22	0.31
3H-1, 19–21	14.09	8	-0.86	-0.03
3H-3, 99–101	17.89	7	-1.29	1.16
3H-4, 59–61	18.99	7	-1.06	0.85
3H-6, 19–21	21.59	6	-1.06	0.75
4H-1, 39–41	23.79	7	-0.99	1.13
4H-2, 139–141	26.29	7	-1.24	0.46
4H-4, 79–81	28.69	7	-1.33	0.36
4H-5, 79–81	30.19	7	-1.22	0.49
5H-1, 79–81	33.69	7	-1.66	1.13
5H-2, 56–58	34.96	7	-1.86	0.8
5H-3, 99–101	35.39	7	-1.72	0.52
5H-4, 119–121	38.59	7	-1.80	0.49
5H-5, 79–81	39.69	7	-1.76	-0.05
5H-6, 59–61	40.99	7	-2.36	0.05
5H-7, 17–19	42.07	7	-2.18	0.02
6H-1, 100–102	43.75	7	-1.07	-0.18
6H-2, 100–102	45.25	8	-0.92	0.13
6H-3, 100–102	46.75	8	-0.61	-0.01
6H-5, 20–22	48.90	8	-0.97	0.23
6H-6, 100–102	51.10	8	-1.85	0.76
6H-CC, 20–22	52.27	7	-2.18	-0.11
7H-3, 20–22	55.65	8	-1.49	0.99
7H-4, 100–102	57.95	8	-1.81	1.21
7H-5, 101–103	59.45	8	-1.45	0.58

transition. Dissolution lags behind the ice-volume record by ~8 k.y., which is the difference between the widely accepted figure of ~18 k.y. for the LGM (Martinson et al., 1987) and ~10 k.y. for the last preservation spike (immediately below Sample 134-828A-2H-1, 29–31 cm). A lag of a similar magnitude exists between the maximum ice-volume of Stage 6 (~135 k.y., per Martinson et al., 1987) and its last preservation spike (125 k.y.). There is a good correspondence between the first peak in dissolution and minimum ice volume. This applies for interglacial Stages 1 and 5, but not necessarily Stage 7.

Furthermore, a pattern of variation of planktonic foraminifers can be seen during intervals of dissolution minima (i.e., that part of the record where percentage variations are reliable and not distorted by dissolution). Such is the case with *G. sacculifer*, which shows increasing values from Stage 6 (glacial maximum) to the Stage 6–5 transition, and from Stage 2 (the LGM) to the Stage 2–1 transition (Fig. 2C). This pattern of variations is opposite to that of the percentage abundance of *Globigerina bulloides* (Fig. 2F). Percentage variations do not exceed 15% and coincide with major variations in the stable isotope record.

Figures 4A and 4B were plotted bearing in mind the distortion of the ice-volume/paleotemperature record (the stable isotope record) and the climatic/paleoecologic signal (the foraminiferal record) caused by dissolution, and the possible reworking through turbidites and/or contourites. Unlike Figure 2, samples near any stratigraphic contact were excluded. The resulting reliability curve, with several species abundances, suggests the existence of short climatic/paleoecologic pulses, the actual meaning of which still needs to be defined or tested. This is the case with the relative drop in abundance of *G. sacculifer* at ~7 mbsf in Hole 828A that perhaps corresponds to the Younger Dryas event recently reported in the Sulu Sea (Linsley and Thunell, 1990; Kudrass et al., 1991) and the Gulf of Carpentaria (De Deckker et al., 1991). It is worth emphasizing here the strong resemblance between

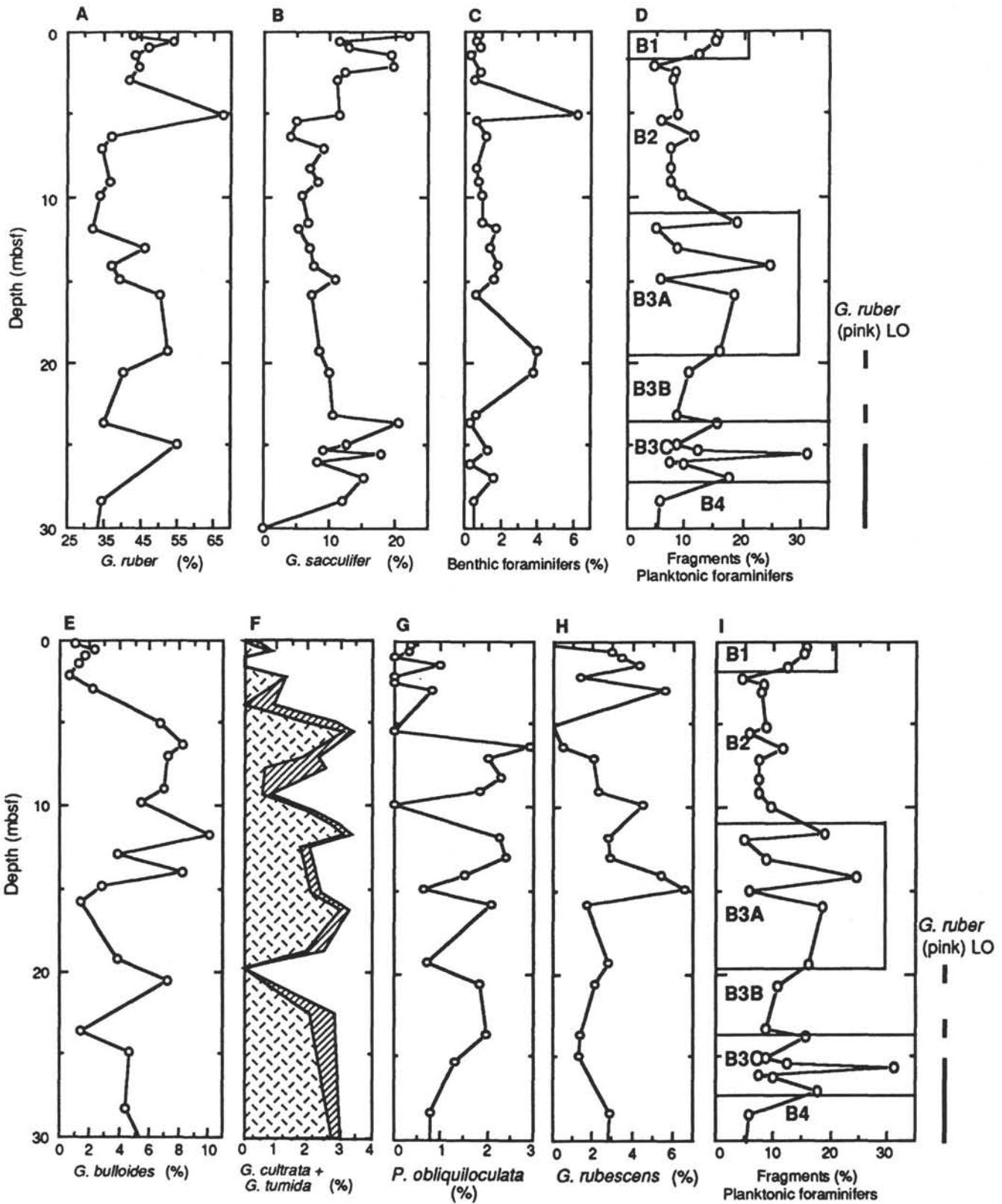


Figure 3. Hole 832A. Percentage variation of selected species of planktonic foraminifers (arranged according to their solution susceptibility) vs. the percentage of benthic foraminifers (C) and planktonic fragmentation (D, I). B1 to B5 refer to dissolution cycles.

Table 4. Planktonic foraminifer fragmentation and three-point moving average for Hole 828A.

Core, section, interval (cm)	Depth (mbsf)	Fragments		Core, section, interval (cm)	Depth (mbsf)	Fragments	
		Percentage	Three-point moving average			Percentage	Three-point moving average
1H-1, 44-46	0.45	37.5	—	3H-3, 119-121	18.09	44.0	31.00
1H-1, 47-48	0.48	27.7	38.10	3H-3, 139-141	18.29	37.0	37.30
1H-1, 106-108	1.07	49.0	38.90	3H-4, 19-21	18.59	31.0	31.00
1H-2, 7-8	1.57	39.9	40.10	3H-4, 39-41	18.79	25.0	27.70
1H-2, 57-58	2.07	31.3	42.80	3H-4, 59-61	18.99	27.0	26.00
1H-2, 115-117	2.65	57.4	39.80	3H-4, 79-81	19.19	26.0	27.90
1H-3, 20-21	3.20	30.8	44.90	3H-4, 99-101	19.39	30.6	27.50
1H-3, 82-83	3.82	46.4	29.60	3H-4, 119-121	19.59	26.0	23.90
2H-1, 9-11	4.49	11.8	21.30	3H-4, 139-141	19.79	15.0	21.60
2H-1, 29-31	4.69	5.7	7.00	3H-5, 19-21	20.09	24.0	25.00
2H-1, 47-49	4.87	3.4	5.20	3H-5, 39-41	20.29	36.0	25.00
2H-1, 69-71	5.09	6.4	5.70	3H-5, 59-91	20.49	15.0	27.00
2H-1, 89-91	5.29	7.4	6.80	3H-5, 79-81	20.69	30.0	23.30
2H-1, 109-111	5.49	6.7	7.20	3H-5, 99-101	20.89	25.0	27.00
2H-1, 129-131	5.69	7.6	6.40	3H-5, 119-121	21.09	26.0	27.00
2H-2, 1-3	5.91	4.9	6.50	3H-5, 139-141	21.29	27.0	29.00
2H-2, 19-21	6.09	6.9	5.60	3H-6, 19-21	21.59	39.0	28.30
2H-2, 39-41	6.29	5.0	6.50	3H-6, 39-41	21.79	21.0	22.10
2H-2, 58-61	6.48	7.5	5.70	3H-6, 59-61	21.99	25.0	24.10
2H-2, 79-81	6.69	4.5	6.30	3H-6, 99-101	22.39	27.0	24.10
2H-2, 99-101	6.89	5.8	5.50	3H-6, 119-121	22.59	25.0	29.30
2H-2, 120-122	7.10	5.1	6.90	3H-6, 139-141	22.79	36.0	34.20
2H-2, 139-141	7.29	8.9	8.00	3H-7, 19-21	23.09	41.5	32.50
2H-3, 9-11	7.49	10.0	8.90	3H-7, 39-41	23.29	20.0	24.80
2H-3, 29-31	7.69	7.8	11.80	3H-7, 58-60	23.48	13.0	23.00
2H-3, 48-50	7.88	17.6	10.70	4H-1, 23-24	23.63	36.0	22.00
2H-3, 69-71	8.09	6.7	12.00	4H-1, 39-41	23.79	17.0	27.70
2H-3, 89-91	8.29	11.6	8.90	4H-1, 59-61	23.99	30.0	23.00
2H-3, 109-111	8.49	8.4	9.10	4H-1, 79-81	24.19	22.0	31.70
2H-3, 129-131	8.69	7.4	9.80	4H-1, 99-101	24.39	43.0	34.70
2H-3, 148-150	8.88	13.5	11.60	4H-1, 119-121	24.59	39.0	33.00
2H-4, 19-21	9.09	14.0	13.30	4H-1, 139-141	24.79	17.0	25.40
2H-4, 39-41	9.29	12.5	13.10	4H-2, 19-21	25.09	20.2	17.70
2H-4, 59-61	9.49	12.9	12.70	4H-2, 39-41	25.29	16.0	21.70
2H-4, 79-81	9.69	12.8	12.80	4H-2, 59-61	25.49	29.0	25.30
2H-4, 99-101	9.89	12.8	13.00	4H-2, 79-81	25.69	31.0	33.67
2H-4, 119-121	10.09	13.4	14.40	4H-2, 99-101	25.89	41.0	31.24
2H-5, 2-4	10.42	16.9	15.70	4H-2, 119-121	26.09	21.7	27.58
2H-5, 20-22	10.60	16.8	16.50	4H-2, 139-141	26.29	20.0	19.91
2H-5, 40-42	10.80	15.9	16.40	4H-3, 19-21	26.59	18.0	15.67
2H-5, 59-61	10.99	16.5	12.20	4H-3, 39-41	26.79	9.0	18.01
2H-5, 79-81	11.19	4.1	14.30	4H-3, 59-61	26.99	27.0	15.01
2H-5, 100-102	11.40	22.4	16.70	4H-3, 79-81	27.19	9.0	16.01
2H-5, 120-122	11.60	23.6	21.20	4H-3, 99-101	27.39	12.0	11.67
2H-5, 140-142	11.80	17.7	20.40	4H-3, 119-121	27.59	14.0	14.00
2H-6, 12-14	12.02	19.8	18.60	4H-3, 139-141	27.79	16.0	18.67
2H-6, 30-32	12.20	18.3	23.30	4H-4, 19-21	28.09	26.0	18.67
2H-6, 48-50	12.38	31.7	23.20	4H-4, 39-41	28.29	14.0	19.00
2H-6, 69-71	12.59	19.5	22.80	4H-4, 59-61	28.49	17.0	24.00
2H-6, 89-91	12.79	17.2	17.80	4H-4, 79-81	28.69	41.0	22.33
2H-6, 110-112	13.00	16.7	20.10	4H-4, 99-101	28.89	9.0	25.02
2H-6, 130-132	13.20	26.3	21.70	4H-4, 119-121	29.09	25.1	16.69
2H-7, 2-4	13.42	22.2	25.70	4H-4, 139-141	29.29	16.0	20.35
2H-7, 22-24	13.62	28.7	27.00	4H-5, 19-21	29.59	20.0	19.67
2H-7, 40-42	13.80	30.2	26.10	4H-5, 39-41	29.79	23.0	26.22
3H-1, 19-21	14.09	19.3	22.80	4H-5, 59-61	29.99	35.7	29.22
3H-1, 39-41	14.29	19.0	19.40	4H-5, 79-81	30.19	29.0	36.56
3H-1, 59-61	14.49	20.0	19.00	4H-5, 99-101	30.39	45.0	33.33
3H-1, 79-81	14.69	18.0	21.30	4H-5, 119-121	30.59	26.0	32.00
3H-1, 99-101	14.89	26.0	32.70	4H-5, 139-141	30.79	25.0	32.75
3H-1, 119-121	15.09	23.0	27.30	4H-6, 19-21	31.09	47.3	37.08
3H-1, 139-141	15.29	33.0	31.00	4H-6, 39-41	31.29	39.0	39.75
3H-2, 19-21	15.59	37.0	33.00	4H-6, 59-61	31.49	33.0	41.00
3H-2, 39-41	15.79	29.0	31.70	4H-6, 79-81	31.69	51.0	47.67
3H-2, 59-61	15.99	29.0	27.00	4H-6, 99-101	31.89	59.0	52.04
3H-2, 79-81	16.19	23.0	25.00	4H-6, 119-121	32.09	46.1	46.37
3H-2, 99-101	16.39	25.0	24.00	4H-6, 139-141	32.29	34.0	40.04
3H-2, 119-121	16.59	26.0	28.00	4H-7, 19-21	32.59	40.0	45.00
3H-2, 139-141	16.79	35.0	28.00	4H-7, 39-41	32.79	61.0	46.74
3H-3, 19-21	17.09	23.0	33.70	4H-CC, 19-21	33.02	39.2	42.07
3H-3, 39-41	17.29	43.0	30.00	5H-1, 19-21	33.09	26.0	32.74
3H-3, 59-61	17.49	24.0	29.30	5H-1, 39-41	33.29	33.0	49.67
3H-3, 79-81	17.69	21.0	19.00	5H-1, 62-64	33.52	57.0	45.00
3H-3, 99-101	17.89	12.0	25.70	5H-1, 79-81	33.69	45.0	42.00

Table 4 (continued).

Core, section, interval (cm)	Depth (mbsf)	Fragments		Core, section, interval (cm)	Depth (mbsf)	Fragments	
		Percentage	Three-point moving average			Percentage	Three-point moving average
5H-1, 99-101	33.89	24.0	34.67	5H-6, 99-101	41.39	55.0	48.00
5H-1, 119-121	34.09	35.0	33.67	5H-6, 119-121	41.59	21.0	38.30
5H-1, 139-141	34.29	42.0	43.33	5H-6, 139-141	41.79	39.0	24.10
5H-2, 19-21	34.59	53.0	47.00	5H-7, 17-19	42.07	12.3	18.77
5H-2, 39-41	34.79	46.0	48.33	5H-7, 39-41	42.29	5.0	8.43
5H-2, 56-58	34.96	46.0	43.73	5H-7, 59-61	42.49	8.0	8.33
5H-2, 79-81	35.19	39.2	40.73	5H-CC, 19-21	42.76	12.0	9.40
5H-2, 99-101	35.39	37.0	50.39	6H-1, 20-22	42.95	8.1	11.67
5H-2, 119-121	35.59	75.0	53.00	6H-1, 100-102	43.75	14.9	12.25
5H-2, 139-141	35.79	47.0	55.10	6H-2, 20-22	44.45	13.7	16.11
5H-3, 19-21	36.09	43.3	46.10	6H-2, 100-102	45.25	19.7	14.81
5H-3, 39-41	36.29	48.0	49.43	6H-3, 20-22	45.95	11.0	13.99
5H-3, 59-61	36.49	57.0	49.67	6H-3, 100-102	46.75	11.3	10.09
5H-3, 79-81	36.69	47.0	49.67	6H-4, 20-22	47.40	8.0	13.67
5H-3, 99-101	36.89	45.0	47.67	6H-4, 100-102	48.20	21.7	13.79
5H-3, 119-121	37.09	51.0	42.33	6H-5, 20-22	48.90	11.6	16.20
5H-3, 139-141	37.29	31.0	38.00	6H-5, 100-102	49.70	15.2	22.90
5H-4, 19-21	37.59	32.0	31.00	6H-6, 17-19	50.10	41.8	30.56
5H-4, 39-41	37.79	30.0	32.33	6H-6, 100-102	51.10	34.6	39.18
5H-4, 60-62	38.00	36.0	32.00	6H-7, 20-22	51.80	41.1	29.89
5H-4, 79-81	38.19	31.0	46.67	6H-CC, 20-22	52.27	14.0	21.58
5H-4, 99-101	38.39	74.0	48.00	7H-1, 21-23	52.65	9.7	12.55
5H-4, 119-121	38.59	39.0	51.33	7H-1, 101-103	53.45	14.0	11.61
5H-4, 139-141	38.79	41.0	40.67	7H-2, 20-22	54.15	11.1	13.63
5H-5, 19-21	39.09	42.0	38.00	7H-2, 101-103	54.95	15.7	16.68
5H-5, 39-41	39.29	31.0	41.67	7H-3, 20-22	55.65	23.2	21.91
5H-5, 59-61	39.49	52.0	40.33	7H-3, 100-102	56.45	26.8	21.80
5H-5, 79-81	39.69	38.0	45.33	7H-4, 20-22	57.15	15.5	25.19
5H-5, 99-101	39.89	46.0	50.65	7H-4, 100-102	57.95	33.3	18.45
5H-5, 119-121	40.09	67.9	61.32	7H-5, 20-22	58.65	6.5	15.52
5H-5, 139-141	40.29	70.0	77.65	7H-5, 101-103	59.45	6.7	8.04
5H-6, 19-21	40.59	95.0	83.00	7H-6, 20-22	60.15	10.9	8.00
5H-6, 39-41	40.79	84.0	75.97	7H-6, 111-113	60.95	6.4	8.08
5H-6, 59-61	40.99	48.9	66.97	7H-7, 16-18	61.62	6.9	—
5H-6, 79-81	41.19	68.0	57.3				

the fragmentation curve and both the CO₂ Antarctic record (Barnola et al., 1987) and the δ¹⁸O record on Ontong Java Plateau (Shackleton and Opdyke, 1976).

The low variation in abundance of some subtropical to transitional (cold water) species, such as *G. bulloides*, *Globorotalia inflata*, and *Globorotalia truncatulinoides* between glacial-interglacial cycles, supports the paleotemperature estimations of Anderson et al. (1989). These authors found that, for the northern part of the Coral Sea, sea-surface temperatures remained constant or changed very slightly between the LGM and the present, viz. 29°C in summer and 27°C in winter, as depicted at Hole RC10-131 located northwest of ODP Holes 828A and 832A (Anderson et al., 1989).

Sedimentation Rates

Figure 5A depicts the inferred average sedimentation rate curve for the upper 62 mbsf interval, drawn on the basis of AMS¹⁴C ages, stable isotope data, and the last occurrence of *G. ruber* (pink variety). Average sedimentation rates increased progressively and dramatically (~10 to ~50 cm/k.y.) as more terrigenous material became available. The significance of this change is discussed below. An additional test to determine the possible influence of turbidites on the fragmentation record was performed by plotting the number of stratigraphic contacts against the mean percentage of fragments in each dissolution-preservation interval (Fig. 6). No correlation appears from this figure, suggesting that turbidites have no significant effect on fragmentation. The number of geologic contacts was obtained from the sedimentological logs (Collot, Greene, Stokking, et al., 1992) and from core photographs. It is certain that with the aid of

additional techniques (e.g., X-ray radiographs) hidden contacts will appear. It is worth emphasizing here that the highest frequency of stratigraphic contacts per meter, and hence the interval of maximum episodic sedimentation of the record, occurs towards the top of Hole 828A, showing a maximum around 10 mbsf (i.e., the LGM).

Sedimentation rates for Hole 832A are slightly lower than those for Hole 828A, based on the only control point available, the last occurrence of *G. ruber* (pink variety) at ~28 mbsf (Fig. 3). Planktonic foraminifers were counted, where possible, at intermittent intervals below 30 mbsf (not illustrated). However, because of the increasing abundance of volcanic ash, no pattern could be determined.

DISCUSSION

Paleoceanography

Dissolution cycles found in Holes 828A and 832A closely resemble the established pattern for the western equatorial Pacific; the two sites are in the southernmost limit of this dissolution regime. Farrell and Prell (1989) showed the modern lysocline to be at approximately 4 km (based on percentage of CaCO₃ in core tops) for the central equatorial Pacific, whereas Parker and Berger (1971) suggested that it is around 3.4 km for the western equatorial Pacific. More recently Wu et al. (1991) proposed that the lysocline fluctuated between 3.6 km during deglacial transitions and 2.6 km during stages of ice growth in the western equatorial Pacific.

Figure 7 shows the modern foraminiferal lysocline profile for the area between 160° and 180°E, and 10° and 30°S (Table 5). Foraminiferal fragmentation from 23 core-top samples were plotted against water depth. Fragmentation above 3.1 km varies between 5% and

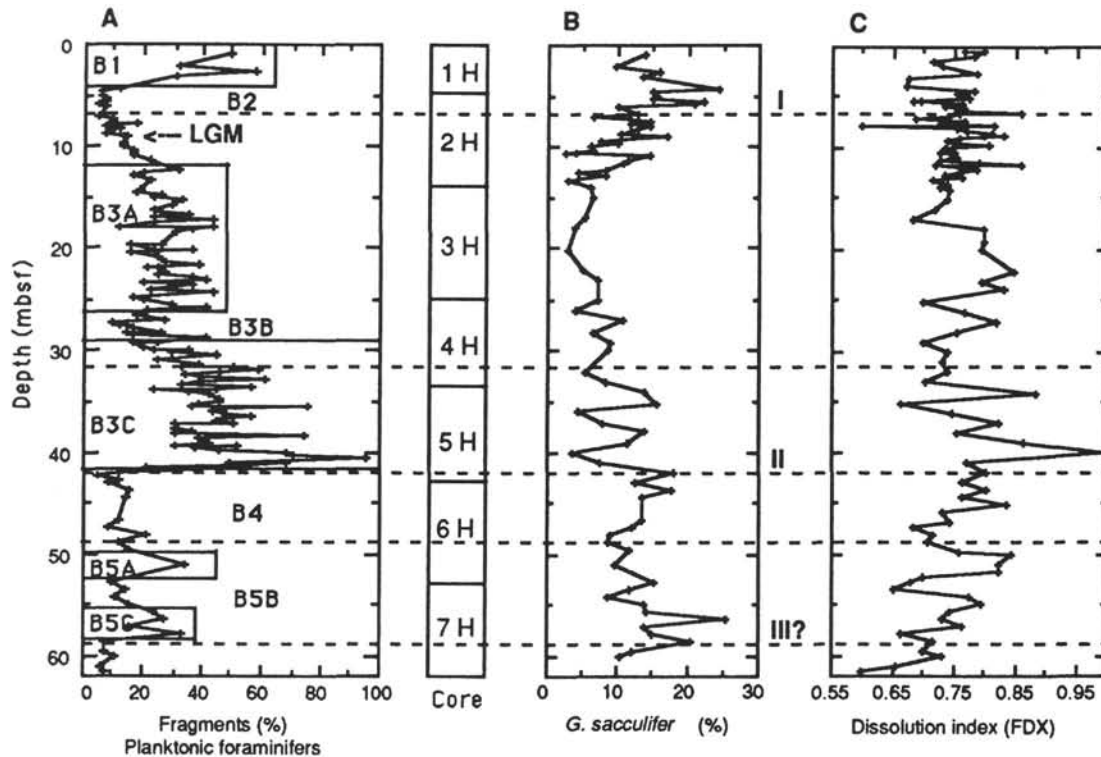


Figure 4. Hole 828A. (A) Percentage of fragments and (B) *G. sacculifer* remaining after the exclusion of those samples close to stratigraphic contacts ("reliability curve"), and (C) the foraminiferal dissolution index $FDX = \sum (P_i R_i) / r_i$.

14%, with 2 anomalous 20% values. Fragmentation below 3.1 km increases dramatically from 22% reaching a maximum of 60%. One anomalous 12% value occurs below 4 km. The lysocline level (3.1 km) marks the water depth where dissolution starts to increase; below 4.25 km some planktonic foraminifers are completely dissolved. The anomalous fragmentation of samples around 2 km possibly results from the presence of a deep oxygen-minimum zone at this level (Wyrski, 1961), higher CO_2 content, and corrosive water. The anomalous sample at about 4 km possibly results from the proximity of the carbonate compensation depth: here dissolution is so intense that fragments of planktonic foraminifers are greatly reduced in size and consequently not retained in the size fraction examined (i.e., $>150 \mu m$). Le and Shackleton (1992) show that the carbonate saturation index (ΔCO_3^{*2}) diminishes below the level where fragmentation increases sharply, and they replot Berger et al.'s (1982) modern lysocline data for the Ontong Java Plateau (their Fig. 5). The carbonate saturation index indicates the degree of calcite saturation in seawater and represents the difference between the in-situ (CO_3^{*2}) of seawater and the saturation (CO_3^{*2}) of calcite (Broecker and Peng, 1982). Le and Shackleton (1992) found very similar results to those shown here (including the anomalous sample at about 4 km), with the lysocline level at 3 km depth. Figure 7 and the work of Le and Shackleton (1992) show that fragmentation is a very sensitive indicator of the lysocline position in the water column. As indicated above, the limits of dissolution intervals in Figure 2 were defined at the 20% fragmentation value, which is somewhat higher than fragmentation percentage above the lysocline in the region (Fig. 7). It follows that the lysocline level was shallower during dissolution intervals, and deeper during preservation intervals. Thus, we can express variations in fragmentation percentage in terms of equivalent water depths, and then infer the lysocline level depth through time. Figure 8B was drawn by comparing average fragmentation percentage from each dissolution interval with fragmentation percentages from the present day lysocline (Fig. 7). Error bars are indicated by shaded areas. Equivalent water depths are

referenced to the present seafloor depth (3086 m) and indicate the relative position of the lysocline level (upper scale on Fig. 8B). Values above the modern lysocline show high error bars; consequently, it is impossible to assess the past lysocline level position (i.e., during intervals of low dissolution). The lower scale in Figure 8B shows the equivalent lysocline variations in the past. Deeper than 3086 m, lysocline levels during intervals of dissolution minima (B2, B3B, B4, and B5B) are indicated only as relative positions, whereas shallower lysocline levels during dissolution maxima (B1, B3A, B3B, B5A, and B5C) range from ~2550 to 3000 m. The average fragmentation value of dissolution Interval B1, when compared with the present-day lysocline profile, suggests that the lysocline level west of Vanuatu is shallower than 3086 m. This indicates that the lysocline profile west of Vanuatu is of the near-continent type, but was of an open ocean type before Termination II (cf. Berger, 1970). The change of the lysocline profile through time may have influenced dissolution intensity and the fragmentation percentage, therefore biasing the position of the inferred lysocline in the past. The wide range of variation of fragmentation percentages during dissolution intervals ("noise" in Fig. 2E) appears to be the normal situation for samples below the lysocline level (see Fig. 7). Differences in sedimentation rate, sediment disturbance (reworking and mixing), and temporal variations in the ΔCO_3^{*2} profile could explain these fluctuations. As indicated above, the fragmentation curve shows an intriguing similarity with the $\delta^{18}O$ stack record (Martinson et al., 1987). This similarity is closer (by eliminating some noise) when comparing the $\delta^{18}O$ record with a 3-point moving average fragmentation curve (Fig. 8A).

Parker and Berger (1971) showed how for the eastern equatorial Pacific upwelling high productivity and consequently high export of organic matter to deep waters enhances dissolution and raises the lysocline (CO_2 in pore waters is produced by oxidation of organic matter). At present, there are no indications of upwelling in the Vanuatu region. However, the Trade Winds may force some offshore movement of water along the western side of Espiritu Santo Island,

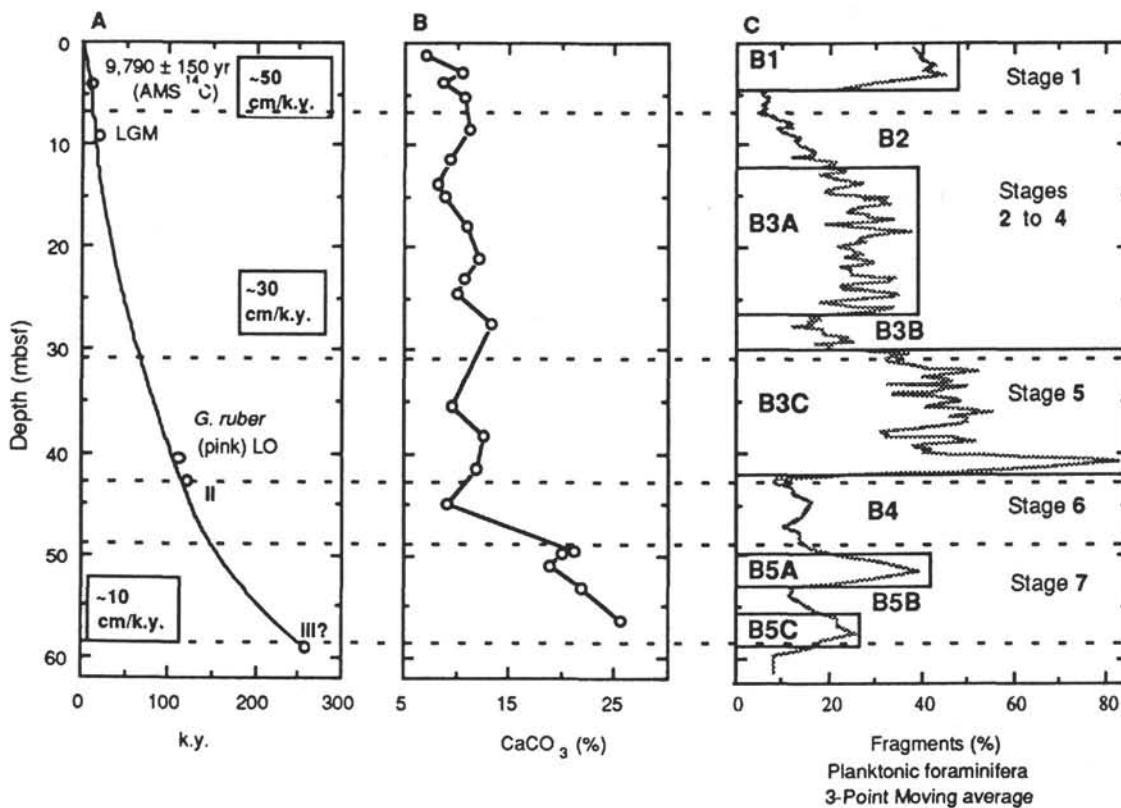


Figure 5. Hole 828A. (A) Average sedimentation rate curve and (B) percentage of CaCO_3 ; (C) the fragmentation curve (3-point moving average) is included for comparison. Isotopic Stages 1 to 7, as well as dissolution Cycles B1 to B5 are indicated.

thus triggering some upwelling. If some productivity blooms did occur, these were greatly diluted by terrigenous material, as shown by the low contents of total organic carbon (TOC up to 0.5%, see Collot, Greene, Stokking, et al., 1992), although TOC may come from wood fragments rather than plankton. As mentioned above, mid-water flows (and turbidites) are an ever-present feature that, together with the common occurrence of woody material, account for the high supply of terrigenous sediments, which may prevent plankton blooms from occurring in the area.

When comparing ODP Hole 828A with Hole V28-238 (collected at 3120 m by Thompson, 1976), a pattern of slightly less fragmentation and small calcium carbonate fluctuations due to dilution by terrigenous material is found. Carbonate cyclicity is the result of an interplay of (1) changes in productivity and rates of sediment fluxes, keeping dissolution rates of carbonate at constant level; (2) flux variations in the ratios of calcareous particles to siliceous particles; (3) changes in dilution by nonbiogenic material such as terrigenous and volcanic particles; and (4) fluctuations in carbonate dissolution (Wu et al., 1991). Quaternary records of carbonate dissolution cycles have been referred to as "periodites" (Einsele, 1982b) because they are of allocyclic origin (i.e., the above-mentioned parameters). In Vanuatu, this periodite pattern has been partially obliterated by terrigenous input. This pattern is shown in Figure 5B (data from Collot, Greene, Stokking, et al., 1992). The sedimentary parameters, bioturbation, and sedimentation rate of the background sediments of turbidites may remain more or less unaffected (Einsele, 1982a), if we assume a simple situation in which we have constant carbonate supply, nonbiogenic supply increasing upwards, and dissolution varying cyclically. Then, from the combination of these three parameters we can expect to see the upward decrease of CaCO_3 with lower values caused by dissolution (cf. Einsele and Ricken, 1991). In Hole 828A this pattern is not evident except, perhaps, for dissolution Interval B1

(Fig. 5B). Carbonate supply and/or nonbiogenic supply must vary accordingly to produce the observed CaCO_3 pattern. Figure 9 shows a semi-quantitative way to explore the influence of the nonbiogenic supply (terrigenous dilution) and dissolution on the CaCO_3 record (Dean et al., 1981; Diester-Haass, 1991). CaCO_3 content has been plotted vs. carbonate dissolution (benthic/[benthic + planktonic foraminifers]) for Hole 828A. It appears that dissolution and dilution increase from Cores 139-828A-7H to -1H. From this figure, however, it is uncertain whether or not carbonate input has varied. Cores 6H and 7H show the lowest degree of dissolution, but increasing dilution. If carbonate supply increased from Core 7H to 1H, then terrigenous input would have favored rather than prevented the bloom of calcareous plankton (foraminifers and nannofossils) in the area. Core 1H shows a maximum in dissolution and dilution whereas Cores 2H to 5H show intermediate values. Berger (1968) and Parker and Berger (1971) based their lysocline models on the gradient of the FDX. FDX values are affected by the interference of the solution ranking with the latitudinal and depth rankings (Berger, 1968). This explains the high dispersion of FDX values in recent lysocline profiles (e.g., Parker and Berger, 1971), as well as those illustrated here (Fig. 4C). Consequently, FDX is of limited value for inferring or constraining lysocline profiles in the past. The same limitations apply to the planktonic foraminiferal susceptibility and to the benthic abundance. These two indicators reflect paleoclimatic and paleoecologic conditions at the sea surface and the seafloor together with dissolution, making them of limited value for inferring lysocline profiles in the past.

Implicitly assume that dissolution occurs at the seafloor. Nonetheless, Thunell and Honjo (1981) showed that substantial foraminiferal solution occurs in the fraction $<150 \mu\text{m}$ during its transit through the water column. According to Berger and Piper (1972), a foraminifer test $100 \mu\text{m}$ in diameter takes approximately 10 to 15 days to descend through 2.5 km of water. In Vanuatu, the travel time of foraminifer

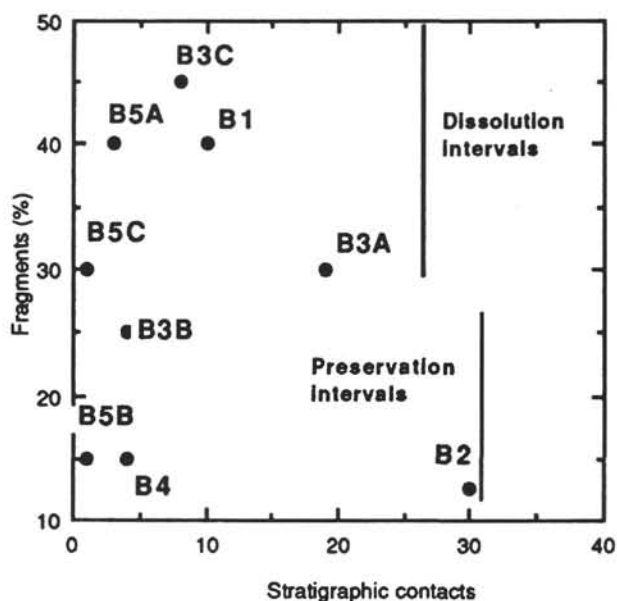


Figure 6. Hole 828A. Percentage of fragments vs. number of stratigraphic contacts. Note the lack of correlation.

tests could take longer because of the presence of a high-salinity layer (~36‰) between 100 and 400 m (Tomczak and Hao, 1989). This longer transit time would favor dissolution.

As indicated above, Hole 828A resembles Pickering's Facies C1.1 and D1.2 (Pickering et al., 1989), indicating that these facies are the product of mud-dominated turbidity currents with "rapid deposition of silt grains and mud flocculations from suspension with no size-sorting either in the viscous sublayer or on the bed." It appears that most of the woody material, and possibly most of the mud, was transported as dilute mid-water flows along a density interface (the pycnocline?) that easily travelled across the trench to reach the NDR (Fig. 10). A simple test applying Stoke's law (Hsü, 1989) seems to support this possibility. Plagioclase ($G = 2.67$) and pyroxene ($G = 3.5$) are common minerals in the silt and very fine sand fraction of Hole 828A (see Collot, Greene, Stokking, et al., 1992). If we use a 100- μ m-diameter particle, a salinity of 36‰, and a temperature of 18°C, then we have a transit time on the order of 10 days for plagioclase and of 7 days for pyroxene to reach the seafloor. In either case descent velocities are lower than 0.5 cm/s. Consequently, oceanic currents can easily keep silt particles, foraminifers, radiolarians, and woody material in suspension as they travel along mid-water flows. Accelerated dropping of these components to the seafloor could be enhanced by the formation of "marine snow." It has been suggested that in areas of high productivity interstitial CO_2 favors the dissolution of planktonic foraminifers (Emerson and Bender, 1980). This mechanism seems to be of lesser importance in this area because the highest content of organic matter coincides with the preservation maxima. The same can be said of the suggested acidity generated by submarine weathering of volcanic ash, which seems to show the opposite pattern in the Vanuatu region: higher content of volcanic ash in Hole 832A coincides with a lower percentage of fragmentation compared to Hole 828A where the content of volcanic ash is minimal.

The above-mentioned time lag of ~8 k.y. for the last glacial-interglacial interval agrees with the estimations of Farrell and Prell (1989) for the central equatorial Pacific. Peterson and Prell (1985) pointed out the differences between the inventory and circulation models to explain both time lags and out-of-phase dissolution patterns between the Atlantic and the Pacific oceans. Inventory models include that of Shackleton (1977) who suggested that preservation-dissolution of

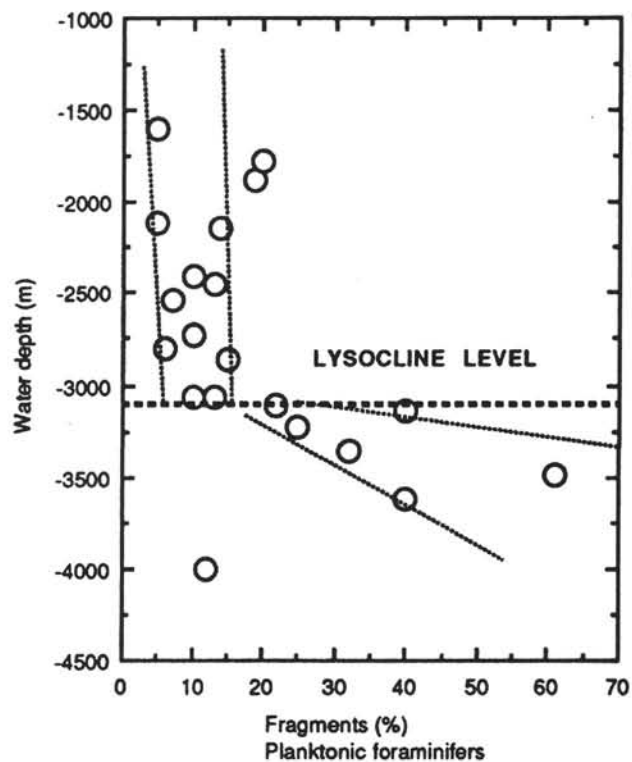


Figure 7. Modern foraminiferal lysocline profile for the area between 160° and 180°E, and 10° and 30°S (see Table 5 for details). Counting error variation ~5%. Note the position of the lysocline level at 3.1 km.

deep sea carbonates is due to the variations of terrestrial biomass during deglaciations and glaciations pumping out and injecting CO_2 in the ocean. Other models include balances of phosphorous and organic carbon between the continental shelves and the deep sea (Broecker, 1982), and the rearrangements of nutrients between intermediate to deep depths during glacial/interglacial transitions (Broecker and Peng, 1987; Boyle, 1988). Circulation models, on the other hand, suggest that variations in the NADW (active only during interglacial intervals) may account for the differences in dissolution patterns between the Atlantic and the Pacific (e.g., Volat et al., 1980). I have mentioned the close similarities between Vanuatu and Ontong Java Plateau. Nonetheless in Hole 828A there is no time lag between ice volume minima and dissolution maxima as shown by Le and Shackleton (1992) for Ontong Java Plateau. Is this difference due to the high-resolution record from Vanuatu? If not, then local phenomena, including CO_2 sinks (see map by Keeling, 1968), and the interplay of different water masses (e.g., the North Pacific vs. the Circumpolar Deep Water; Shackleton, 1985) could explain the difference, rather than carbonate supply variations that apparently were minor. In any case, dissolution of planktonic foraminifers in Hole 828A apparently responded (linearly?) to changes in atmospheric CO_2 as recorded in the polar regions (e.g., Barnola et al., 1987). A satisfactory mechanism still must be proposed to explain this relationship and the out-of-phase record between fragmentation and stable isotope curves.

Tectonic Implications

The pattern of sedimentation rates of Hole 828A can be explained by the progressive migration of the NDR toward Espiritu Santo Island. If we accept the present spreading rates of ~13 cm/yr as constant, then the NDR was approximately 32 km away from the New Hebrides Trench 250 ka, 16 km at 120 ka, and 2.3 km at 18 ka (Fig. 10).

Table 5. List of data used to calculate the modern lysocline for the Vanuatu region. Planktonic foraminiferal fragmentation data on 23 core-tops.

Core	Position		Water depth (m)	Foraminiferal fragmentation (%)
	Latitude	Longitude		
NOVA-A 53	28°16'S	161°31'E	1607	5
RC10-139	03°02'S	156°26'E	1781	20
RC12-115	22°05'S	173°16'E	1875	19
RC13-39	15°53'S	176°50'E	2116	5
NOVA-A 36	21°41'S	167°23'E	2148	14
RC12-103	26°00'S	179°44'E	2401	10
RC12-113	24°53'S	163°31'E	2454	13
RC9-124	28°14'S	172°36'E	2540	7
RC12-117	16°25'S	174°30'E	2734	10
RC13-40	17°24'S	176°41'E	2798	6
RC13-38	14°31'S	177°06'E	2867	15
RC13-37	11°52'S	177°25'E	3067	13
NOVA-H 20	12°53'S	176°39'E	3063	10
RC12-107	26°00'S	169°12'E	3115	22
RC12-116	19°28'S	175°06'E	3136	40
RC12-118	12°59'S	174°01'E	3233	25
RC12-108	26°02'S	165°49'E	3354	32
NOVA-HV 15	28°10'S	171°12'E	3489	61
NOVA-A 40	23°00'S	164°58'E	3617	40
RC12-114	24°46'S	170°26'E	3997	12
RC12-104	26°04'S	176°42'E	4330	0
RC12-105	26°04'S	176°42'E	4356	0
RC12-106	26°01'S	174°01'E	4669	0

Note: Counting error ~5%, on the >149 μm size fraction.

As subduction progressed, the sedimentation regime changed from pelagic to hemipelagic over the NDR. Turbiditic clouds moving as mid-water flows reached the site about 125 ka, releasing their silt, clay, and woody material load. The existence at present of a salinity maximum layer (~36‰) between 100 to 400 m (Tomczak and Hao, 1989) supports this interpretation as strong density contrasts favor the existence of mid-water flows (Pickering et al., 1989). Bottom turbidites apparently were not effective until later when Site 828 approached the New Hebrides Trench. This event coincided with the LGM when the eustatic drop in sea level favored the high-energy erosion of the island, and worldwide oceanic conditions were more dynamic (higher storm activity). At this time, turbidite clouds were able to bypass the New Hebrides Trench and terrigenous input became important. The increase in sedimentation rates appears to result from both proximity to, and upheaval of, the island.

CONCLUSIONS

1. Pelagic to hemipelagic sediments of the uppermost 61.9 m of Hole 828A were deposited during isotopic Stages 7 to 1 (~250 ka to present). The high-resolution pattern of foraminiferal fragmentation in Hole 828A shows the record of dissolution Intervals B1 to B5C. This record is very similar to the $\delta^{18}\text{O}$ stack (Martinson et al., 1987) and the atmospheric record of CO_2 as recorded in ice cores (Barnola et al., 1987) and is out of phase with the $\delta^{18}\text{O}$ record of *G. sacculifer*.

2. Comparing dissolution minima and maximum ice volume, the dissolution record is lagging the isotopic record by approximately 8 k.y. in accord to previous studies for the equatorial Pacific (e.g., Farrell and Prell, 1989). No lag was found between dissolution maxima and minimum ice volumes (different from the Ontong Java Plateau where a 6- to 20-k.y. lag has been recorded, Le and Shackleton, 1992). Local CO_2 sinks and the interplay between intermediate and deep water masses may explain the difference.

3. Fragmentation of planktonic foraminifers is a more sensitive dissolution indicator than planktonic foraminiferal susceptibility, the foraminiferal dissolution index (Berger, 1968), the abundance of benthic foraminifers, and CaCO_3 content. A modern lysocline for the area is found at 3.1 km below sea level (foraminiferal lysocline)

compared to west of Vanuatu where it is shallower (a near continent type). A 20% threshold in foraminiferal fragmentation indicates past lysocline fluctuations.

4. The past lysocline was deeper (than 3086 m) during intervals of dissolution minima, and ranged from ~2550 to 3000 m during intervals of dissolution maxima.

5. Site 828 is progressively affected by mid-water flows and turbidites that become important from 125 ka to present. Dilution by terrigenous material affected the lysocline profile that evolved from an open ocean to a near continent type.

6. The very high sedimentary record found in Hole 828A opens new and interesting possibilities for high-resolution paleoceanographic and paleoclimatic studies, either in this hole or on further localities west of this site where turbidites must occur in lower proportion. This equally applies to analogous seaward trench localities all over the world previously considered as unsuitable for this type of study (Ruddiman, 1977).

7. The complete $\delta^{18}\text{O}$ record of Hole 828A is expected to provide a more precise chronostratigraphic framework and new insights into dissolution cyclicality.

ACKNOWLEDGMENTS

I thank Dr. Patrick De Deckker for scientific advice and for critical review of the manuscript. Dr. John Tipper made valuable suggestions and Dr. Richard Gillespie prepared samples for AMS and arranged the datings at DSIR (Nuclear Science Group, New Zealand). Dr. Allan Chivas and Mr. Joe Cali performed the stable isotope analyses at the Research School of Earth Sciences (The Australian National University). Dr. Jörn Thiede kindly provided the core-top samples. Thoughtful reviews of the manuscript by Drs. John Chappell, André Droxler, Gary Greene, Michael Ayress, and an anonymous reviewer are greatly appreciated. I wish to acknowledge the financial help of the Australian ODP secretariat (Dr. Tony Crawford) to participate on Leg 134 and to attend the post-cruise meeting. This paper is part of my Ph.D. thesis project on the paleoceanography of the southwest Pacific during the Brunhes Chron (Australian National University Ph.D. scholarship).

REFERENCES*

- Anderson, D.M., Prell, W.L., Barratt, N.J., 1989. Estimates of sea surface temperature in the Coral Sea at the Last Glacial Maximum. *Paleoceanography*, 4:615-627.
- Arrhenius, G., 1952. Sediment cores from the east Pacific. *Rep. Swed. Deep-Sea Exped. 1947-1948*, 5.
- , 1988. Rate of production, dissolution and accumulation of biogenic solids in the ocean. *Palaeogeogr. Palaeoclimatol., Palaeoecol.*, 67:119-146.
- Bard, E., Hamelin, B., Fairbanks, R.G., and Zinder, A., 1990. Calibration of the ^{14}C time-scale over the past 30,000 years using mass spectrometric U-Th ages from Barbados corals. *Nature*, 345:405-410.
- Barnola, J.M., Raynaud, D., Korotkevich, Y.S., and Lorius, C., 1987. Vostok ice core provides 160,000-year record of atmospheric CO_2 . *Nature*, 329:408-414.
- Bé, A.W.H., 1977. An ecological, zoogeographic and taxonomic review of Recent planktonic foraminifera. In Ramsay, A.T.S. (Ed.), *Oceanic Micropaleontology* (Vol. 1): London (Academic Press), 1-100.
- Berger, W.H., 1968. Planktonic foraminifera: selective solution and paleoclimatic interpretation. *Deep-Sea Res. Part A*, 15:31-43.
- , 1970. Planktonic foraminifera: selective solution and the lysocline. *Mar. Geol.*, 8:111-138.
- , 1977. Deep-sea carbonate and deglaciation preservation spike in pteropods and foraminifera. *Nature*, 269:301-304.
- Berger, W.H., Bonneau, M.-C., and Parker, F.L., 1982. Foraminifera on the deep-sea floor: lysocline and dissolution rate. *Oceanol. Acta*, 5:249-258.

* Abbreviations for names of organizations and publications in ODP reference lists follow the style given in *Chemical Abstracts Service Source Index* (published by American Chemical Society).

- Berger, W.H., and Killingley, J.S., 1977. Glacial-Holocene transition in deep-sea carbonates: selective dissolution and the stable isotope signal. *Science*, 197:563–566.
- Berger, W.H., and Piper, D.J.W., 1972. Planktonic foraminifera: differential settling, dissolution and redeposition. *Limnol. Oceanogr.*, 17:275–287.
- Boyle, E.A., 1988. Vertical oceanic nutrient fractionation and glacial/interglacial CO₂ cycles. *Nature*, 331:55–56.
- Broecker, W.S., 1971. Calcite accumulation rates and glacial to interglacial changes in oceanic mixing. In Turekian, K.K. (Ed.), *The Late Cenozoic Glacial Ages*: New Haven, CT (Yale Univ. Press), 239–265.
- , 1982. Glacial to interglacial changes in ocean chemistry. *Prog. Oceanogr.*, 11:151–197.
- Broecker, W.S., and Peng, T.H., 1982. *Tracers in the Sea*: New York (Lamont-Doherty Geological Observatory, Columbia Univ.).
- , 1987. The role of CaCO₃ compensation in the glacial to interglacial atmospheric CO₂ change. *Global Biogeochem. Cycles*, 1:15–29.
- Broecker, W.S., Trumbore, S., Bonani, G., Wolfi, W., and Klas, M., 1989. Anomalous AMS radiocarbon ages for foraminifera from high-deposition-rate ocean sediments. *Radiocarbon*, 31:157–162.
- CLIMAP Project Members, 1981. Seasonal reconstructions of the Earth's surface at the last glacial maximum. *Geol. Soc. Am., Map and Chart Ser.*, MC36:1–18.
- Collot, J.-Y., Greene, H.G., Stokking, L.B., et al., 1992. *Proc. ODP, Init. Repts.*, 134: College Station, TX (Ocean Drilling Program).
- Dean, W.E., Gardner, J.V., and Cepek, P., 1981. Tertiary carbonate-dissolution cycles on the Sierra Leone Rise, eastern Equatorial Atlantic Ocean. *Mar. Geol.*, 39:81–101.
- De Deckker, P., Corregge, T., and Head, J., 1991. Late Pleistocene record of cyclic eolian activity from tropical Australia suggesting the Younger Dryas is not an unusual event. *Geology*, 19:602–605.
- Diester-Haass, L., 1991. Rhythmic carbonate content variations in Neogene sediments above the oceanic lysocline. In Einsele, G., Ricken, W., and Seilacher, A. (Eds.), *Cycles and Events in Stratigraphy*: Berlin (Springer-Verlag), 94–109.
- Dimberline, A.J., and Woodcock, N.H., 1987. The southwest margin of the Wenlock turbidite system, Mid-Wales. *Geol. J.*, 22:61–71.
- Dott, R.H., Jr., 1983. Episodic sedimentation—How normal is average? How rare is rare? Does it matter? *J. Sediment. Petrol.*, 53:5–23.
- Einsele, G., 1982a. General remarks about the nature, occurrence, and recognition of cyclic sequences (periodites). In Einsele, G., and Seilacher, A. (Eds.), *Cyclic and Event Stratification*: Berlin (Springer-Verlag), 3–7.
- , 1982b. Limestone-marl cycles (periodites): diagnosis, significance, causes—a review. In Einsele, G., and Seilacher, A. (Eds.), *Cyclic and Event Stratification*: Berlin (Springer-Verlag), 8–53.
- Einsele, G., and Ricken, W., 1991. Limestone-marl alternation—an overview. In Einsele, G., Ricken, W., and Seilacher, A. (Eds.), *Cycles and Events in Stratigraphy*: Berlin (Springer-Verlag), 23–47.
- Emerson, S., and Bender, M., 1981. Carbon fluxes at the sediment-water interface of the deep-sea: calcium carbonate preservation. *J. Mar. Res.*, 39:139–162.
- Emery, W.J., and Meincke, J., 1986. Global water masses: summary and review. *Oceanol. Acta*, 9:383–391.
- Erez, J., Almogi-Labin, A., and Avraham, S., 1991. On the life history of planktonic foraminifera: lunar reproduction cycle in *Globigerinoides sacculifer* (Brady). *Paleoceanography*, 6:295–306.
- Farrell, J.W., and Prell, W.L., 1989. Climatic change and CaCO₃ preservation: an 800,000 year bathymetric reconstruction from the central equatorial Pacific Ocean. *Paleoceanography*, 4:447–466.
- Gray, W.M., 1968. Global view of the origin of tropical disturbances and storms. *Mon. Weather Rev.*, 96:669–700.
- Hays, J.D., Saito, T., Opdyke, N.D., and Burckle, L.H., 1969. Pliocene-Pleistocene sediments of the equatorial Pacific: their paleomagnetic, biostratigraphic, and climatic record. *Geol. Soc. Am. Bull.*, 80:1481–1513.
- Howarth, R., and Greene, G., 1991. Effects of cyclones Ursula, Carlotta and Uma in the Port Villa-Mele Bay area, Vanuatu. In *Workshop on Water Processes in the South Pacific Island Nations, Lae, Papua New Guinea*, 1–8 October 1987. SOPAC Tech. Bull., 7:123–124.
- Hsü, K., 1989. *Physical Principles of Sedimentology*: Berlin (Springer-Verlag).
- Huang, T.C., 1980. A volcanic sedimentation model: implication of processes and responses of deep-sea ashes. *Mar. Geol.*, 38:103–122.
- Keeling, C.D., 1968. Carbon dioxide in surface ocean waters, 4: Global distributions. *J. Geophys. Res.*, 14:4543–4553.
- Kudrass, H.R., Erlenkeuser, H., Vollbrecht, R., and Weiss, W., 1991. Global nature of the Younger Dryas cooling event inferred from oxygen isotope data from Sulu Sea cores. *Nature*, 349:406–409.
- Le, J., and Shackleton, N.J., 1992. Carbonate dissolution fluctuations in the western equatorial Pacific during the late Quaternary. *Paleoceanography*, 7:21–42.
- Linsley, B.K., and Thunell, R.C., 1990. The record of deglaciation in the Sulu Sea: evidence for the Younger Dryas event in the western tropical Pacific. *Paleoceanography*, 5:1025–1039.
- Luz, B., 1973. Stratigraphic and paleoclimatic analysis of Late Pleistocene tropical southeast Pacific cores. *Quat. Res. (N.Y.)*, 3:56–72.
- Luz, B., and Shackleton, N.J., 1975. CaCO₃ solution in the tropical east Pacific during the past 130,000 years. *Spec. Publ. Cushman Found. Foraminiferal Res.*, 13:142–150.
- Martinson, D.G., Pisias, N.G., Hays, J.D., Imbrie, I., Moore, T.C., Jr., and Shackleton, N.J., 1987. Age dating and the orbital theory of the ice-ages: development of a high-resolution 0 to 300,000-year chronostratigraphy. *Quat. Res. (N.Y.)*, 27:1–29.
- Moore, T.C., Burckle, L.H., Geitzenauer, K., Luz, B., Molina-Cruz, A., Robertson, J.H., Sachs, H., Sancetta, C., Thiede, J., Thompson, P., and Wenkam, C., 1980. The reconstruction of sea surface temperatures in the Pacific Ocean of 18,000 BP. *Mar. Micropaleontol.*, 5:215–247.
- Moore, T.C., Pisias, N.G., and Heath, G.R., 1977. Climate changes and lags in Pacific carbonate preservation, sea surface temperature and global ice volume. In Malahoff, A., and Anderson, N. (Eds.), *The Fate of Fossil Fuel CO₂ in the Oceans*: New York (Plenum), 145–165.
- Parker, F.L., and Berger, W.H., 1971. Faunal and solution patterns of planktonic Foraminifera in surface sediments of the South Pacific. *Deep-Sea Res. Part A*, 18:73–107.
- Peterson, L.C., and Prell, W.L., 1985. Carbonate preservation and rates of climatic change: an 800 kyr record from the Indian Ocean. In Sundquist, E.T., and Broecker, W.S. (Eds.), *The Carbon Cycle and Atmospheric CO₂: Natural Variations Archean to Present*: Am. Geophys. Union Monogr., 32:251–270.
- Pickering, K.T., Hiscott, R.N., and Hein, F.J., 1989. *Deep Marine Environments: Clastic Sedimentation and Tectonics*: London (Unwin Hyman).
- Rotschi, H., and Lemasson, L., 1967. Oceanography of the Coral and Tasman Seas. *Oceanogr. Mar. Biol.*, 5:49–97.
- Ruddiman, W.F., 1977. Investigations of Quaternary climate based on planktonic Foraminifera. In Ramsay, A.T.S. (Ed.), *Oceanic Micropaleontology*: New York (Academic Press), 1:101–162.
- Shackleton, N.J., 1977. Carbon-13 in *Uvigerina*: tropical rainforest history and the equatorial Pacific carbonate dissolution cycles. In Andersen, N.R., and Malahoff, A. (Eds.), *The Fate of Fossil Fuel CO₂ in the Oceans*: New York (Plenum), 401–427.
- , 1985. Formation of bottom water in the glacial North Pacific. *Eos*, 66:292.
- Shackleton, N.J., and Opdyke, N.D., 1973. Oxygen isotope and paleomagnetic stratigraphy of equatorial Pacific core V28-238: oxygen isotope temperatures and ice volumes on a 10⁵ year and 10⁶ year scale. *Quat. Res. (N.Y.)*, 3:39–55.
- , 1976. Oxygen-isotope and paleomagnetic stratigraphy of Pacific Core V28-239: late Pliocene to latest Pleistocene. In Cline, R.M., and Hays, J.D. (Eds.), *Investigations of Late Quaternary Paleoclimatology and Paleoclimatology*. Mem.—Geol. Soc. Am., 145:449–464.
- Thompson, P.R., 1976. Planktonic foraminiferal dissolution and the progress towards a Pleistocene equatorial Pacific transfer function. *J. Foraminiferal Res.*, 6:208–227.
- Thompson, P.R., Duplessy, J.C., and Bé, A.H., 1979. Disappearance of pink-pigmented *Globigerinoides ruber* at 120,000 yr BP in the Indian and Pacific Oceans. *Nature*, 280:554–558.
- Thompson, P.R., and Saito, T., 1974. Pacific Pleistocene sediments: planktonic foraminifera dissolution cycles and geochronology. *Geology*, 2:333–335.
- Thunell, R.C., 1976. Optimum indices of calcium carbonate in deep-sea sediments. *Geology*, 4:525–528.
- Thunell, R.C., and Honjo, S., 1981. Planktonic foraminiferal flux to the deep ocean: sediment trap results from the tropical Atlantic and the central Pacific. *Mar. Geol.*, 40:237–253.
- Thunell, R.C., Qingmin, M., Calvert, S.E., and Pedersen, T.F., 1992. Glacial-Holocene biogenic sedimentation patterns in the South China Sea: productivity variations and surface water pCO₂. *Paleoceanography*, 7:143–162.

- Tomczak, M., and Hao, D., 1989. Water masses in the thermocline of the Coral Sea. *Deep-Sea Res. Part A*, 36:1503–1514.
- Volat, J.-L., Pastouret, L., and Vergnaud-Grazzini, C., 1980. Dissolution and carbonate fluctuations in Pleistocene deep-sea cores: a review. *Mar. Geol.*, 34:1–28.
- Wu, G., and Berger, W.H., 1989. Planktonic foraminifera: differential dissolution and the Quaternary stable isotope record in the west-equatorial Pacific. *Paleoceanography*, 4:181–198.
- Wu, G., Herguera, J.C., and Berger, W.H., 1990. Differential dissolution: modification of late Pleistocene oxygen isotope records in the western equatorial Pacific. *Paleoceanography*, 5:581–594.

- Wu, G., Yasuda, M.K., and Berger, W.H., 1991. Late Pleistocene carbonate stratigraphy on Ontong-Java Plateau in the western equatorial Pacific. *Mar. Geol.*, 99:135–150.
- Wyrki, K., 1962. The subsurface water masses in the western South Pacific Ocean. *Aust. J. Mar. Freshwater Res.*, 13:18–47.

Date of initial receipt: 2 April 1992

Date of acceptance: 19 November 1992

Ms 134SR-012

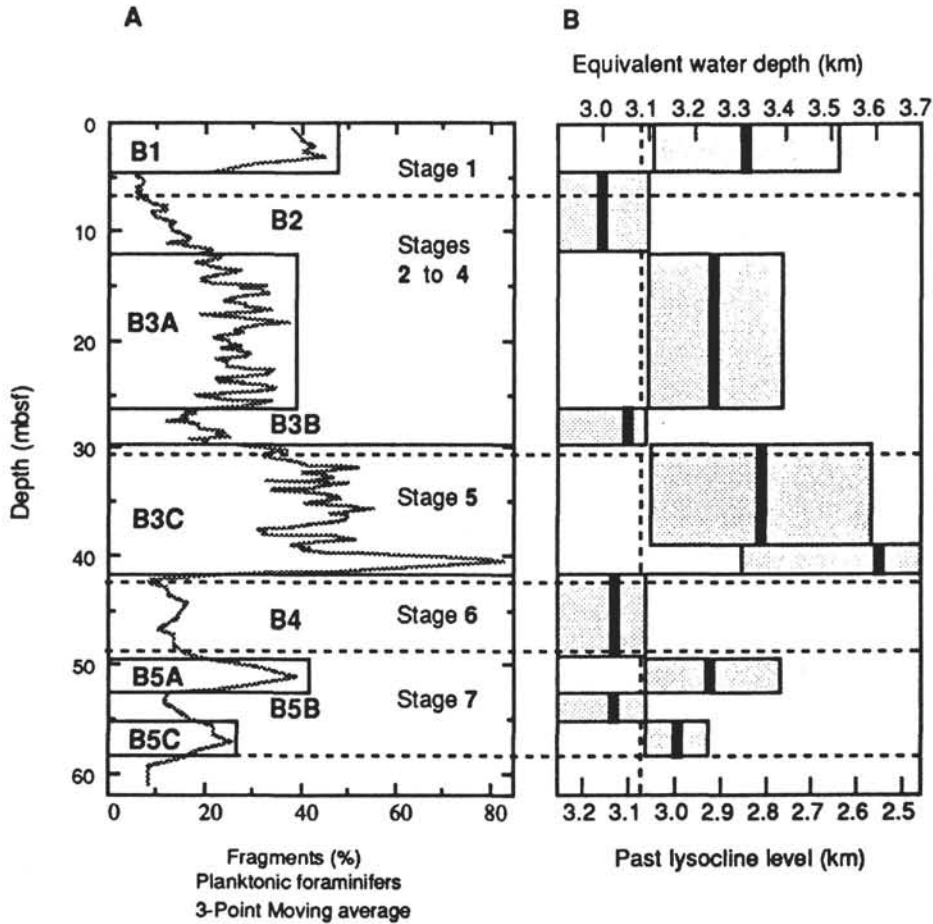


Figure 8. Hole 828A. (A) Percentage of fragments (3-point moving average) vs. (B) equivalent water depth (upper scale) and the lysocline level in the past (lower scale). Shaded areas indicate error bars; black lines indicate the approximate position of the lysocline level. Error bars on the left of the present seafloor depth (dashed line) extend to at least 1.5 km (see Fig. 7 for comparison). Lysocline level positions for preservation intervals are uncertain and indicated only as relative values.

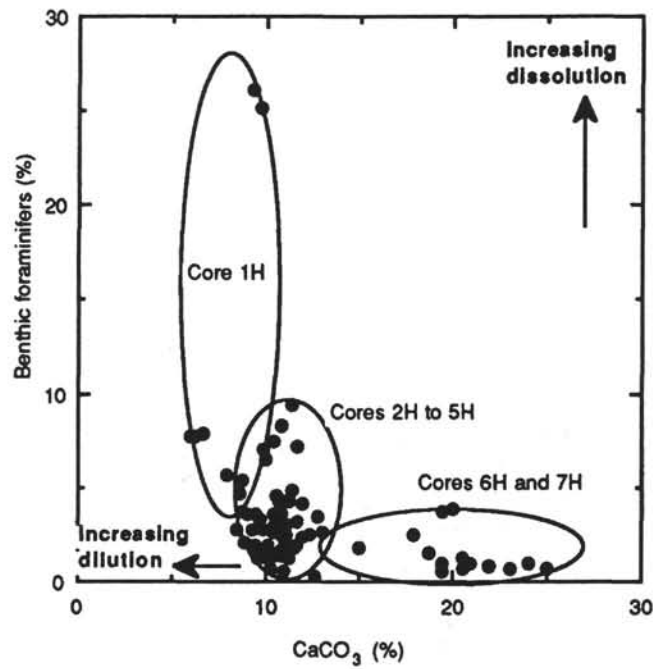


Figure 9. Hole 828A. Calcium carbonate content vs. carbonate dissolution (percentage of benthic foraminifers expressed as benthic/[benthic + planktonic foraminifers]). Note increasing dilution and dissolution effects from Core 139-828A-7H to -1H.

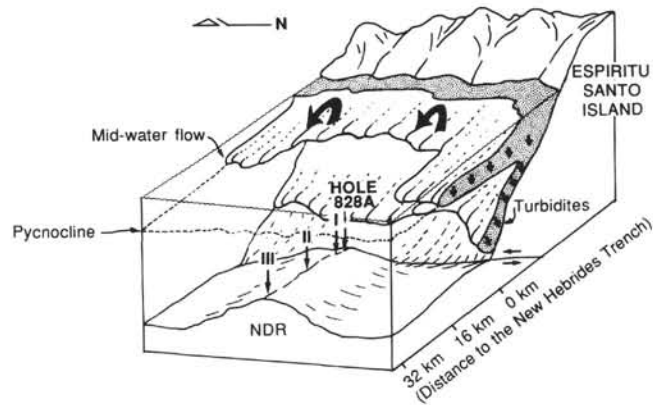


Figure 10. Hole 828A. Sedimentation model for western Vanuatu. The paleo-location of Site 828 is illustrated at three different times: Termination III, II, and I, when the distance to the trench was ~32, ~16, and ~2.4 km, respectively. Mid-water flows, activated by the frequent storms of the area, moved along a density contrast (the high-salinity layer found between 100 and 400 m). True turbidites appear to affect Site 828 around Termination I. Sedimentation model adapted from a drawing by Dimberline and Woodcock (1987).